THE JOURNAL OF BIOLOGICAL CHEMISTRY
Vol. 272, No. 14, Issue of April 4, pp. 9587–9596, 1997
Printed in U.S.A.

Cytotoxic Necrotizing Factor 1 from *Escherichia coli* and Dermonecrotic Toxin from *Bordetella bronchiseptica* Induce p21^{rho}-dependent Tyrosine Phosphorylation of Focal Adhesion Kinase and Paxillin in Swiss 3T3 Cells*

(Received for publication, December 23, 1996)

Hadriano M. Lacerda‡§, Gill D. Pullinger¶, Alistair J. Lax‖, and Enrique Rozengurt‡**

From the ‡Imperial Cancer Research Fund, P. O. Box 123, 44 Lincoln's Inn Fields, London WC2A 3PX, United Kingdom, the ‖UMDS Guy's and St. Thomas's Medical and Dental School, Floor 28 Guy's Tower, Guy's Hospital, London SE1 9RT, United Kingdom, and the ¶Department of Chemical Endocrinology, St. Bartholomews Hospital Medical College, 51-53 Bartholomews Close, London EC1A 7BE, United Kingdom

Treatment of Swiss 3T3 cells with cytotoxic necrotizing factor 1 (CNF1) from *Escherichia coli* and dermonecrotic toxin (DNT) from *Bordetella bronchiseptica*, which directly target and activate p21^{rho}, stimulated tyrosine phosphorylation of focal adhesion kinase (p125^{fak}) and paxillin. Tyrosine phosphorylation induced by CNF1 and DNT occurred after a pronounced lag period (2 h), and was blocked by either lysosomotrophic agents or incubation at 22 °C. CNF1 and DNT stimulated tyrosine phosphorylation of p125^{fak} and paxillin, actin stress fiber formation, and focal adhesion assembly with similar kinetics. Cytochalasin D and high concentrations of platelet-derived growth factor disrupted the actin cytoskeleton and completely inhibited CNF1 and DNT induced tyrosine phosphorylation. Microinjection of *Clostridium botulinum* C3 exoenzyme which ADP-ribosylates and inactivates p21^{rho} function, prevented tyrosine phosphorylation of focal adhesion proteins in response to either CNF1 or DNT. In addition, our results demonstrated that CNF1 and DNT do not induce protein kinase C activation, inositol phosphate formation, and Ca^{2+} mobilization. Moreover, CNF1 and DNT stimulated DNA synthesis without activation of p42^{mapk} and p44^{mapk} providing additional evidence for a novel p21^{rho}-dependent signaling pathway that leads to entry into the S phase of the cell cycle in Swiss 3T3.

An increase in the tyrosine phosphorylation of the non-receptor protein tyrosine kinase p125^{fak} (1, 2) and the cytoskeletal associated protein paxillin (3, 4) has recently been identified as an early event in the action of diverse signaling molecules that mediate cell growth and differentiation (5), including mitogenic neuropeptides (6–8), growth factors such as PDGF[1] (9, 10), bioactive lipids (11–15), extracellular matrix proteins (16–20), transforming variants of pp60^{src} (17, 21), and the potent mitogenic toxin PMT (22). p125^{fak} lacks SH2 and SH3 domains but associates with other proteins including Src, paxillin, and p130^{cas} (1, 2, 23). Paxillin is a multidomain protein that may function as an adaptor capable of complex formation with p125^{fak}, Crk, Src, and vinculin (3, 4, 23). Gene disruption experiments indicate a critical role of p125^{fak} in embryonic development and cell locomotion (24). The increases in p125^{fak} and paxillin tyrosine phosphorylation are accompanied by profound alterations in the organization of the actin cytoskeleton and in the assembly of focal adhesions (9, 13, 15, 25, 26), the distinct areas of the plasma membrane where p125^{fak} and paxillin are localized (1, 2, 27). The small G protein p21^{rho}, a member of the Ras superfamily of small GTP-binding proteins, has been implicated in the mitogen-stimulated formation of focal adhesions and actin stress fibers as well as in the tyrosine phosphorylation of p125^{fak} and paxillin (22, 25, 28–30). These findings suggest the existence of a distinct signal transduction pathway in which p21^{rho} is upstream of cytoskeletal reorganization and tyrosine phosphorylation of focal adhesion proteins (5).

The mechanism of action of bacterial toxins has provided novel insights into the control of cellular regulatory processes, including signal transduction and cell proliferation. For example, the *Clostridium botulinum* C3 exoenzyme and the enterotoxins A and B from *Clostridium difficile* which selectively inactivate members of the Rho subfamily, have provided useful tools to evaluate the role of these small G proteins in signal transduction and cytoskeletal organization (31–33). In contrast to these clostridial toxins, CNF toxins produced by some pathogenic strains of *Escherichia coli* (34) and DNT from *Bordetella bronchiseptica* (35) directly target and activate p21^{rho} (36, 37). CNF and DNT induce actin reorganization and multinucleation in several cell types (37–40) but their effects on signal transduction pathways, specially on p125^{fak} and paxillin tyrosine phosphorylation have not been examined.

Here we report that CNF1 and DNT stimulate tyrosine phosphorylation of p125^{fak} and paxillin and induce a concomitant increase in the formation of actin stress fibers and in the assembly of focal adhesion plaques in Swiss 3T3 cells. Microinjection of C3 exoenzyme prevented both the cytoskeletal responses and the increase in tyrosine phosphorylation of focal adhesion proteins. In contrast to most other stimuli that promote tyrosine phosphorylation of p125^{fak} and paxillin (6–15,

* The costs of publication of this article were defrayed in part by the payment of page charges. This article must therefore be hereby marked "*advertisement*" in accordance with 18 U.S.C. Section 1734 solely to indicate this fact.

§ Recipient of Research Fellowship from CNPq-Conselho Nacional de Desenvolvimento Cientifico e Tecnologico Brasilia, Brasil.

** To whom all correspondence should be addressed. Tel.: 44-0171-269-3455; Fax: 44-0171-269-3417.

[1] The abbreviations used are: PDGF, platelet-derived growth factor; PMT, *Pasteurella multocida* toxin; CNF, cytotoxic necrotizing factor; DNT, dermonecrotic toxin; anti-Tyr(P), anti-phosphotyrosine; DMEM, Dulbecco's modified Eagle's medium; mAb, monoclonal antibody; PBS, phosphate-buffered saline; p125^{fak}, p125 focal adhesion kinase; PKC, protein kinase C; MAPK, mitogen-activated protein kinase; PAGE, polyacrylamide gel electrophoresis; Ins(1,4,5)P_3, inositol 1,4,5-trisphosphate; PtdIns(4,5)P_2, phosphatidylinositol 4,5-bisphosphate; FITC, fluorescein isothiocyanate; MARCKS, myristoylated alanine-rich C-kinase substrate.

22), CNF1 and DNT do not activate phospholipase C-mediated events including inositol phosphate production, Ca^{2+} mobilization, and PKC activation. In addition, CNF1 and DNT both stimulated reinitiation of DNA synthesis but neither induce activation of $p42^{mapk}$ (ERK2). Thus, our results demonstrating that CNF1 and DNT induce a specific subset of molecular and cytoskeletal responses in Swiss 3T3 cells provide novel evidence for the existence of a signal transduction pathway that links $p21^{rho}$ activation to tyrosine phosphorylation of focal adhesion proteins.

EXPERIMENTAL PROCEDURES

Cell Culture—Stock cultures of Swiss 3T3 fibroblasts were maintained in DMEM supplemented with 10% fetal bovine serum in a humidified atmosphere containing 10% CO_2 and 90% air at 37 °C. For experimental purposes, cells were plated either in 30-mm Nunc Petri dishes at 10^5 cells/dish, or in 90-mm dishes at 6×10^5 cells/dish, in DMEM containing 10% fetal bovine serum and used after 6–8 days when the cells were confluent and quiescent (41).

DNA Synthesis Measurements—Quiescent cultures of Swiss 3T3 cells were washed twice with DMEM and incubated with DMEM/Waymouth's medium 1:1 (v/v) containing [^{3}H]thymidine (1 μCi/ml) and various factors as indicated. After 40 h, the cultures were washed twice with ice-cold phosphate-buffered saline and incubated in 5% trichloroacetic acid for 30 min at 4 °C. Trichloroacetic acid was then removed and the cultures were washed twice with ethanol and extracted in 1 ml of 2% Na_2CO_3, 0.1 M NaOH, 1% SDS. Incorporation of [^{3}H]thymidine was determined by scintillation counting in 6 ml of scintillation fluid. The proportion of cells in the G_0/G_1, S, G_2, and M phases of the cell cycle were determined by fluorescence-activated cell sorter analysis as described previously (42).

Immunoprecipitation—Quiescent cultures of Swiss 3T3 cells ($1–2 \times 10^6$) were washed twice with DMEM, treated with CNF1, DNT, or PMT or other factors in 10 ml of DMEM/Waymouth (1:1, v/v) for the times indicated and lysed at 4 °C in 1 ml of a lysis buffer solution containing 10 mM Tris/HCl, pH 7.6, 5 mM EDTA, 50 mM NaCl, 30 mM sodium pyrophosphate, 50 mM sodium fluoride, 100 μM Na_3VO_4, and 1% Triton X-100. Proteins were immunoprecipitated at 4 °C overnight with agarose-linked mAbs directed against phosphotyrosine, paxillin, or $p125^{fak}$ as indicated. Immunoprecipitates were washed three times with lysis buffer and extracted for 10 min at 95 °C in 2 × SDS-PAGE sample buffer (200 mM Tris-HCl, 6% SDS, 2 mM EDTA, 4% 2-mercaptoethanol, 10% glycerol, pH 6.8) and analyzed by SDS-PAGE.

Western Blotting—Treatment of quiescent cultures of cells with factors, cell lysis, and immunoprecipitations were performed as described above. After separation by SDS-PAGE, proteins were transferred to Immobilon membranes (43). Membranes were blocked using 5% nonfat dried milk in PBS, pH 7.2, and incubated for 3–5 h at 22 °C with PY72 or 4G10 anti-Tyr(P) mAbs (1 μg/ml). Immunoreactive bands were visualized using ^{125}I-labeled sheep anti-mouse IgG followed by autoradiography. Autoradiograms were scanned using an LKB Ultrascan XL internal integrator. The values expressed represent percentages of the maximum increase in tyrosine phosphorylation above control values.

^{32}P Labeling of Cells and Analysis of 80K/MARCKS Phosphorylation—Quiescent and confluent cultures of Swiss 3T3 cells in 30-mm dishes were washed twice in phosphate-free DMEM and incubated at 37 °C with this medium containing 50 μCi/ml carrier-free [^{32}P]P_i. After 12 h, various factors were added for the indicated times. The cells were subsequently lysed and the lysates were immunoprecipitated with specific anti-80K/MARCKS antibody (44).

Analysis of Total Inositol Phosphates—Cultures of Swiss 3T3 cells in 33-mm dishes were labeled for 16–18 h in 1 ml of DMEM/Waymouth's medium (1:1) containing 10 μCi of [2-^{3}H]inositol. Additions were made to the cells as described for each experiment and LiCl was added to a final concentration of 20 mM for the last 30 min of the incubation. Inositol phosphates were extracted by replacing the medium with 1 ml of ice-cold 3% $HClO_4$. After 20 min at 4 °C the extract was neutralized with 0.5 M KOH containing 25 mM HEPES, 5 mM EDTA, and 0.01% phenol red. Precipitated $KClO_4$ was removed by centrifugation. Analysis of total inositol phosphates was by anion-exchange column chromatography (45). Samples were diluted to 10 ml with water and then loaded onto 1 ml of Dowex AG1-X8 (100–200 mesh, $HCOO^-$ form) in Bio-Rad Econo-columns. After 3 washes with 3×10 ml of H_2O and 2×10 ml of 60 mM NH_4COOH, 5 mM $Na_2B_4O_7$ the inositol phosphates were eluted with 7 ml of 1 M NH_4COOH, 0.1 M HCOOH. An aliquot (1 ml) of eluate was counted in 10 ml of scintillation fluid.

Intracellular Concentration of Ca^{2+}—To determine the intracellular concentration of Ca^{2+}, $[Ca^{2+}]_i$, 5×10^5 cells were subcultured with 10 ml of DMEM containing 10% fetal bovine serum in 90-mm Nunc dishes. After 6–8 days, when the cells were confluent and quiescent, the medium was replaced with 5 ml of DMEM/Waymouth's medium (1:1). The cells were pretreated as indicated, and then 5 μl of 1 mM fura-2/AM (46–48) was added directly to the medium. After a further 10 min the cells were washed twice at 37 °C with 3 ml of electrolyte solution, comprising 140 mM NaCl, 5 mM KCl, 1.8 mM $CaCl_2$, 0.9 mM $MgCl_2$, 25 mM glucose, 16 mM HEPES, 6 mM Tris, pH 7.2, and the amino acid content of DMEM. The cells were then gently removed from the dish by scraping into 2 ml of the electrolyte solution. The cell suspension was transferred to a 1-cm^2 quartz cuvette and stirred at 37 °C for 4 min prior to any additions. Fluorescence was measured in a Perkin-Elmer LS-5 fluorometer with an excitation wavelength of 510 nm. $[Ca^{2+}]_i$ was calculated from the maximum and minimum fluorescence of the fura-2, as described (46, 49).

Immunostaining of Cells—Quiescent Swiss 3T3 cells were washed twice with DMEM and incubated for the indicated times in DMEM/Waymouth's medium (1:1, v/v) at 37 °C with CNF1, DNT, or PMT. For actin staining, cells were washed once with PBS, fixed in 4% paraformaldehyde in PBS for 10 min at room temperature, and permeabilized with PBS containing 0.2% Triton X-100 for 8 min at room temperature. The cells were then incubated with FITC-conjugated phalloidin (0.25 μg/ml) in PBS for 30 min at room temperature and visualized using a Zeiss Axiophot immunofluorescence microscope. In experiments in which quiescent Swiss 3T3 cells were labeled with both FITC-conjugated phalloidin and anti-vinculin antibody, the cells were fixed and permeabilized as described above and then stained with a mixture of FITC-conjugated phalloidin (0.25 μg/ml) and anti-vinculin antibody (dilution 1:100) for 30 min at room temperature. Cells were subsequently washed three times in PBS and then incubated with Cy3-labeled rabbit anti-mouse IgG as a secondary antibody at a dilution of 1:100 for another 30 min at room temperature.

Microinjection of C3 Exoenzyme—For microinjection experiments Swiss 3T3 cells were plated in 33-mm Nunc Petri dishes at 10^5 cells/dish in DMEM containing 10% fetal bovine serum and used after 6–8 days when the cells were confluent and quiescent. Approximately 50 cells were microinjected with 100 μg/ml recombinant C3 exoenzyme. The efficiency of injection was determined by co-injecting guinea pig immunoglobulin at 0.5 mg/ml followed by staining with FITC-linked goat anti-guinea pig IgG. A single batch of C3 transferase was used in all experiments described.

Confocal Microscopy—Confocal imaging was performed using a Bio-Rad MRC 600 laser scanning head fitted to a Nikon Optiphot microscope. A 60X N.A./1.4 planapochromat oil immersion lens (Nikon) was used for all imaging. FITC-conjugated phalloidin and Cy3 anti-mouse IgG fluorochromes were excited at 488 and 568 nm, respectively, using a krypton/argon mixed gas laser (Bio-Rad). Two filter blocks were used, K1 and K2. K1 is a double dichromic filter enabling excitation at the wavelengths of 488 and 568 nm, whereas the K2 filter is a 560-nm dichromic combined with 522-nm green emission and 585-nm red emission filters. Images were collected using the Kalman filter. Care was taken to ensure that the FITC-conjugated phalloidin channel was sufficiently bright relative to the fluorescein signal to minimize the contribution of bleed-through from the green channel into the red channel (approximately 10%). Correction of images for bleed-through and other processing was carried out using COMOS and SOM programs (Bio-Rad) run on a Compaq Deskpro 66M 486 computer (66 MHz). Data are presented as projections of sequential optical sections. For Z-series, optical sections were recorded at 0.5-μm intervals. Final images were photographed directly from the VDU screen.

Shift Assay for MAP Kinase Activation—Activation of $p42^{mapk}$ and $p44^{mapk}$ was determined by the appearance of slower migrating forms in gel electrophoresis due to phosphorylation of specific threonine and tyrosine residues (50). Lysates from quiescent cells in 33-mm dishes prepared as above were subjected to SDS-PAGE and transferred to Immobilon membranes. Membranes were blocked using 5% nonfat dried milk in phosphate-buffered saline. Rabbit polyclonal antibodies raised against COOH-terminal peptides (EETARFQPGYRS for $p42^{mapk}$ and IFQETARFQPGAPE for the $p44^{mapk}$) were used at 1/1000 dilution, and ^{125}I-protein A was used to visualize immunoreactive bands.

Constructs Bearing CNF1, DNT, and PMT—Strain pISS392 is *E. coli* DH5α containing plasmid pISS392 which consists of a 3.5-kilobase fragment encoding only CNF1 inserted into the vector pGEM3. Control strain pGEM3 is *E. coli* DH5α containing a plasmid derived from pISS392 by deletion of a 3.5-kilobase insert. It is pGEM3 with a deletion in the multiple cloning site. Strain DNT1 is *E. coli* XL1-Blue containing

plasmid pDNT1 which consists of a 5-kilobase fragment encoding the DNT gene (*B. bronchiseptica* B58) inserted into the vector pBluescript. Control strain pBlue is *E. coli* XL1-Blue with plasmid pBluescript (51). Strain pTOX2 is *E. coli* XL1-Blue with plasmid pTOX2 which consists of the vector pBluescript with an approximately 4-kilobase pair insert encoding PMT. Control strain pBlue is *E. coli* XL1-Blue with plasmid pBluescript here nominated PC12.

Preparation of Samples of CNF1, DNT, and PMT—The *E. coli* strains were grown overnight from a fresh colony. They were lysed in the lysis buffer (50 μg/ml lysozyme, 5 mM EDTA, 0.1% toluene, 0.05 M Tris-Cl, pH 7.2, 0.1 M NaCl) treated with RNase and DNase at 10 μg/ml each to remove nucleic acid and filtered through a 0.2-μm nitrocellulose filter.

Materials—Bombesin, cytochalasin D, FITC-conjugated phalloidin, monoclonal anti-vinculin mAb, Cy3-linked anti-mouse IgG, guinea pig IgG, and FITC-conjugated goat anti-guinea pig IgG were obtained from Sigma. Recombinant PDGF (BB homodimer), ^{125}I-sheep anti-mouse IgG (15 mCi/mg), carrier-free [^{32}P]P_i, and [2-^{3}H]inositol (18.8 Ci/mmol, 1 Ci = 37 GBq) were all supplied by Amersham Corp., United Kingdom. Agarose-linked anti-Tyr(P) mAb was purchased from Oncogene Science Inc., New York. 4G10 anti-Tyr(P) mAb was from UBI, Lake Placid, NY. mAb 2A7 directed against p125^{fak} was from TCS Biologicals Ltd., Buckingham, United Kingdom. p125^{fak} immunoblotting was performed with mAb from Transduction Laboratories, Lexington, KY. The anti-Tyr(P) mAb PY72 was obtained from the hybridoma development unit, Imperial Cancer Research Fund. Clone pISS392 was kindly supplied by Dr. A. Caprioli, Instituto Superiore di Sanita, Rome, Italy. All other reagents were of the highest grade commercially available. The C3 *C. botulinum* exoenzyme was a gift from Dr. N. Morii and Professor S. Narumiya, Department of Pharmacology, Kyoto University Faculty of Medicine, Sakyo-ku 606, Japan.

RESULTS

CNF1 Stimulates Tyrosine Phosphorylation of p125^{fak} and Paxillin in Swiss 3T3 Cells—To examine the effects of CNF1 on tyrosine phosphorylation, quiescent cultures of Swiss 3T3 cells were treated with the control bacterial lysate (pGEM3) or with lysate containing CNF1 for 6 h. Cell extracts were immunoprecipitated with anti-Tyr(P) mAb followed by Western blotting with an anti-Tyr(P) mAb. As shown in Fig. 1*A*, CNF1 markedly stimulated the tyrosine phosphorylation of a group of bands migrating with an apparent M_r of 110,000–130,000 and 70,000–80,000.

The pattern of tyrosine-phosphorylated proteins induced by CNF1 is similar to that stimulated by bombesin, bioactive lipids, and PMT in Swiss 3T3 cells (8, 13, 15, 22). The cytosolic tyrosine kinase p125^{fak} and the adaptor protein paxillin have been identified as prominent tyrosine-phosphorylated proteins in Swiss 3T3 cells treated with these agents. To determine whether these cellular proteins were also substrates for CNF1-induced tyrosine phosphorylation, extracts from Swiss 3T3 cells, incubated with the control bacterial lysate (pGEM3) or CNF1 for 6 h, were immunoprecipitated with mAbs that recognize either p125^{fak} or paxillin, and the immunoprecipitates were analyzed by Western blotting with anti-Tyr(P) mAb. As shown in Fig. 1*A*, CNF1 markedly stimulated tyrosine phosphorylation of p125^{fak} and paxillin in Swiss 3T3 cells. The control bacterial lysate (pGEM3) did not stimulate tyrosine phosphorylation of these bands or of any other protein (data not shown).

CNF1 Enters the Cell to Transiently Stimulate Tyrosine Phosphorylation of p125^{fak} and Paxillin—Neuropeptides and lysophosphatidic acid induce tyrosine phosphorylation of p125^{fak} and paxillin within minutes of treatment (6, 8, 13), whereas there is a lag period of 1 h between the addition of PMT and a detectable increase in tyrosine phosphorylation of these proteins (22). As shown in Fig. 1*B*, CNF1-stimulated tyrosine phosphorylation of p125^{fak} and paxillin occurred after a lag period of 2 h, reached a maximum after 8 h of treatment and declined to 56% ± 9.5 (mean ± S.E.) of the maximum after 24 h. This is in contrast to the tyrosine phosphorylation of p125^{fak} and paxillin stimulated by PMT which remains maximal after 24 h of treatment (data not shown). Immunoblotting

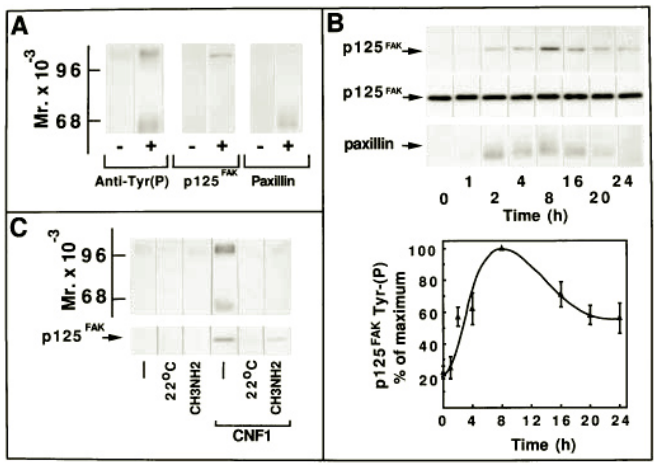

FIG. 1. **CNF1 induces tyrosine phosphorylation of multiple bands including p125^{fak} and paxillin in Swiss 3T3 cells.** *A*, quiescent cultures of Swiss 3T3 cells were treated in DMEM/Waymouth's medium (1:1, v/v) with (−) 5 μg/ml control bacterial lysate (pGEM3) or with (+) 5 μg/ml bacterial lysate containing CNF1 for 6 h. Cells were lysed and the lysates were immunoprecipitated with agarose-linked anti-Tyr(P) mAb, anti-p125^{fak} mAb 2A7, or anti-paxillin mAb 165. The immunoprecipitates were fractionated by SDS-PAGE and further analyzed by immunoblotting with a mixture of anti-Tyr(P) mAbs. *B*, quiescent cultures of Swiss 3T3 cells were treated in DMEM/Waymouth's medium (1:1, v/v) with 5 μg/ml bacterial lysate containing CNF1 for various times (0–24 h) as indicated. Cells were lysed and the lysates were immunoprecipitated using anti-p125^{fak} mAb 2A7 or anti-paxillin mAb and analyzed by immunoblotting with a mixture of anti-Tyr(P) mAbs (*upper* and *lower autoradiograms*). Immunoblotting with p125^{fak} mAb of anti-p125^{fak} immunoprecipitates verified that similar amounts of p125^{fak} were recovered after different times of CNF1 treatment (*middle autoradiogram*). The positions of p125^{fak} and paxillin are indicated by *arrowheads*. The plot shows the values of the mean of three independent experiments which are expressed as the percentage of the maximum stimulation of tyrosine phosphorylation of p125^{fak} band at the indicated times quantified by scanning densitometry. *C*, quiescent cultures of Swiss 3T3 cells were incubated for 6 h in DMEM/Waymouth's (1:1, v/v) medium containing 5 μg/ml bacterial lysate containing CNF1 with or without 10 mM CH_3NH_2 or incubated at 22 °C. Cells were lysed and the lysates immunoprecipitated with anti-Tyr(P) mAb or anti-p125^{fak} mAb 2A7. The immunoprecipitates were fractionated by SDS-PAGE and further analyzed by anti-Tyr(P) immunoblotting. The results shown in this and subsequent figures are representative autoradiographs of at least three independent experiments.

with p125^{fak} mAb of anti-p125^{fak} immunoprecipitates prepared in parallel with those used for the assays of tyrosine phosphorylation verified that similar amounts of p125^{fak} were recovered after different times of CNF1 treatment (Fig. 1*B*).

Next we examined whether the lag period in CNF1 action reflects a requirement for internalization and activation of the toxin during transit through endosomal/lysosomal compartments. The lysosomotrophic agent methylamine, a membrane-permeant weak base known to inhibit lysosomal processing, completely blocked tyrosine phosphorylation of the M_r 110,000–130,000 and M_r 70,000–80,000 bands in response to CNF1 (Fig. 1*C*). Methylamine also prevented the increase in tyrosine phosphorylation of p125^{fak} in response to CNF1 (Fig. 1*C*). The inhibitory effect of methylamine was selective because it did not prevent the increase in tyrosine phosphorylation induced by bombesin in parallel cultures (data not shown). It is also known that the entry of many bacterial toxins into the cell cytoplasm is temperature-dependent. Treatment of Swiss 3T3 cells with CNF1 for 6 h at 22 °C failed to induce tyrosine phosphorylation (Fig. 1*C*). In contrast, bombesin stimulated tyrosine phosphorylation of M_r 110,000–130,000 and M_r 70,000–80,000 bands in parallel cultures incubated at 22 °C (data not shown). Therefore, CNF1 appears to enter cells via an endosomal/lysosomal pathway where it is processed and re-

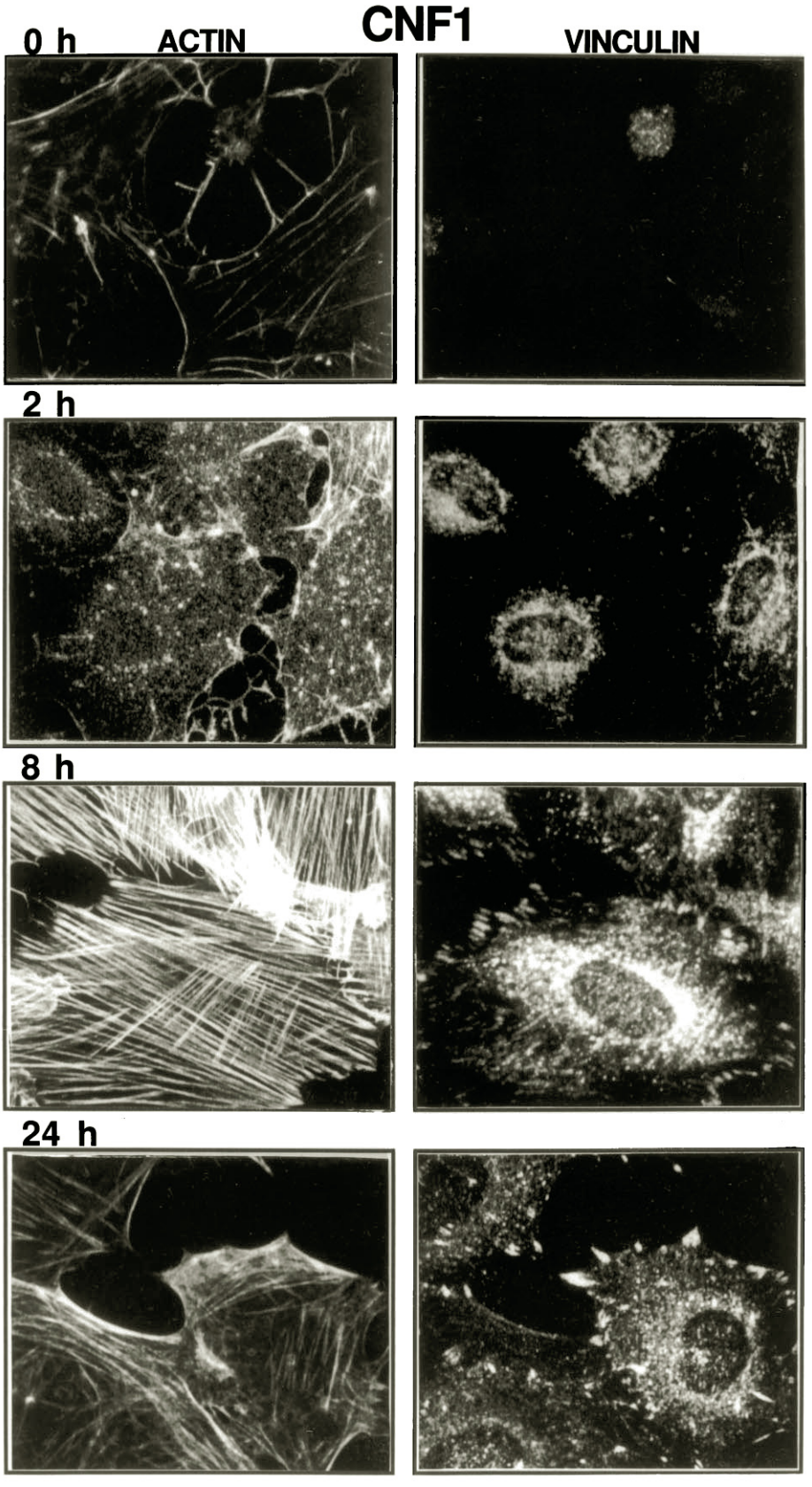

FIG. 2. **Effect of CNF1 on the actin cytoskeleton and focal contacts.** Quiescent cultures of Swiss 3T3 cells were washed with DMEM and incubated in DMEM/Waymouth's medium (1:1, v/v) containing 5 μg/ml lysate containing CNF1 for the times indicated, and then washed with PBS, fixed in 3.7% paraformaldehyde, and permeabilized with 0.2% Triton X-100. A double labeling technique with FITC-conjugated phalloidin and the monoclonal anti-vinculin antibody was used to compare the concomitant changes in the formation of stress fibers with those of vinculin at the focal adhesions (*left* and *right*, respectively). Confocal imaging was performed as described under "Experimental Procedures."

leased into the cytosol in an active form to stimulate tyrosine phosphorylation of $p125^{fak}$ and paxillin.

CNF1 Transiently Induces Actin Stress Fiber Formation and Focal Contact Assembly—Given the localization of $p125^{fak}$ and paxillin to focal contacts which form at the end of actin stress fibers we examined the kinetics of actin cytoskeleton reorganization and focal adhesion assembly induced by CNF1. As shown in Fig. 2, CNF1 treatment of Swiss 3T3 cells induced the formation of new actin stress fibers after a 2-h lag period. Actin reorganization reached a maximum after 8 h of exposure to

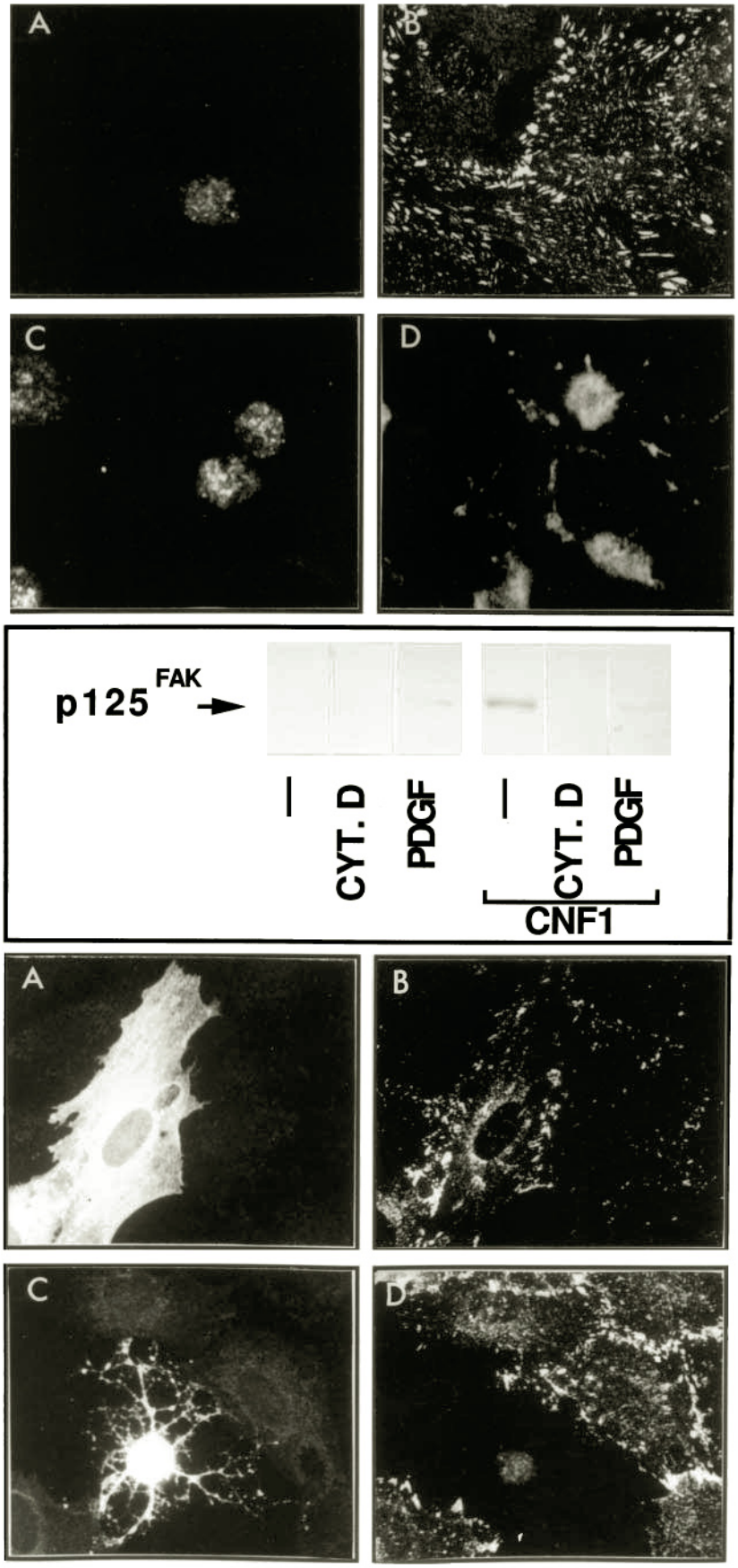

FIG. 3. **Effect of cytochalasin D, PDGF, and C3 exoenzyme on CNF1-stimulated tyrosine phosphorylation and focal adhesion assembly.** *Upper panel,* effect of cytochalasin D and PDGF on CNF1-stimulated focal adhesion assembly. Cells were treated with (*A*) 5 μg/ml control bacterial lysate (pGEM3) for 4 h, (*B*) 5 μg/ml of bacterial lysate containing CNF1 for 4 h, (*C*) 1.2 μM cytochalasin D (*CYT.D*) for 1 h and subsequently with 5 μg/ml bacterial lysate containing CNF1 for 4 h, or (*D*) 5 μg/ml bacterial lysate containing CNF1 for 4 h and 30 ng/ml PDGF for a further 10 min. Cells were then washed with PBS and fixed in 4% paraformaldehyde, permeabilized, and focal adhesion were then visualized with mouse anti-vinculin mAb and Cy3-conjugated rabbit anti-mouse IgG. *Middle panel*, effect of cytochalasin D and PDGF on CNF1 stimulated p125^{fak} tyrosine phosphorylation. Quiescent Swiss 3T3 cells were treated with (−) 5 μg/ml of the control bacterial lysate (pGEM3) or treated with 1.2 μM cytochalasin D for 1 h and then incubated with 5 μg/ml bacterial lysate containing CNF1 for a further 4 h. Parallel cell cultures were treated with 5 μg/ml bacterial lysate containing CNF1 for 4 h and subsequently with 30 ng/ml PDGF for a further 10 min. Cells were then lysed, and the lysates were further analyzed by immunoprecipitation using mAb 2A7 directed against p125^{fak} followed by anti-Tyr(P) Western blotting. *Lower panel,* microinjection of C3 exoenzyme prevents the increase of tyrosine phosphorylation of focal adhesion proteins. Quiescent cultures of Swiss 3T3 cells in 30-mm dishes were washed twice and incubated in DMEM/Waymouth's medium (1:1, v/v). Cells were microinjected with 0.5 mg/ml guinea pig IgG (*A* and *B*) or 0.5 mg/ml guinea pig IgG + 100 μg/ml C3 exoenzyme (*C* and *D*). Cells were then treated with 5 μg/ml bacterial lysate containing CNF1. After 4 h of incubation, the cells were stained with 4G10 mAb directed against phosphotyrosine residues and visualized by confocal microscopy using Cy3-linked rabbit anti-mouse IgG (*B* and *D*). Microinjected cells (shown in *A* and *C*) were identified by staining with FITC-conjugated goat anti-guinea pig IgG Ab.

CNF1. Interestingly, after 24 h of CNF1 treatment, the number of actin stress fibers decreased and actin appeared to accumulate in a cortical fashion. Vinculin staining showed the recruitment of this protein to focal adhesions formed at the ends of actin stress fibers. The number of focal adhesions also reached a maximum after 8 h and decreased after 24 h treatment (Fig.

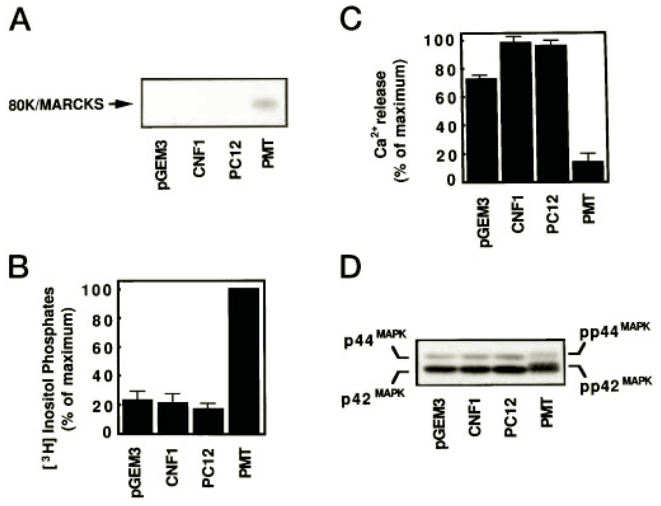

FIG. 4. **CNF1 does not induce PKC activation, inositol phosphate production, Ca^{2+} mobilization, or $p42^{mapk}$/$p44^{mapk}$ activation.** *A*, quiescent cells, labeled with 50 μCi/ml [^{32}P]P_i for 18 h, were treated with 5 μg/ml control bacterial lysate (pGEM3), 5 μg/ml bacterial lysate containing CNF1, 2 μg/ml control bacterial lysate (PC12), or 2 μg/ml bacterial lysate containing PMT and incubated for further 6 h. Cells were subsequently lysed and the lysates were immunoprecipitated with anti-80K/MARCKS antibody and further analyzed by SDS-PAGE. *B*, cells were prelabeled with 10 μCi/ml [2-^{3}H]inositol for 16 h treated with the same conditions as described above adding directly to the dishes and the cultures were incubated at 37 °C for 6 h. LiCl (20 mM) was then added, and after a further 30 min the cellular inositol phosphate content was determined. *C*, $[Ca^{2+}]_i$ was measured as described under "Experimental Procedures." Quiescent cells were pretreated with 5 μg/ml control bacterial lysate (pGEM3), 5 μg/ml bacterial lysate containing CNF1, 2 μg/ml control bacterial lysate (PC12), or 2 μg/ml bacterial lysate containing PMT for 4 h, and the increase in $[Ca^{2+}]_i$ induced by bombesin (10 nM) was then determined. *D*, quiescent cells were treated for 4 h as described above and lysed. The cell extracts were subjected to SDS-PAGE, followed by Western blotting with anti-$p42^{mapk}$/$p44^{mapk}$ antibody.

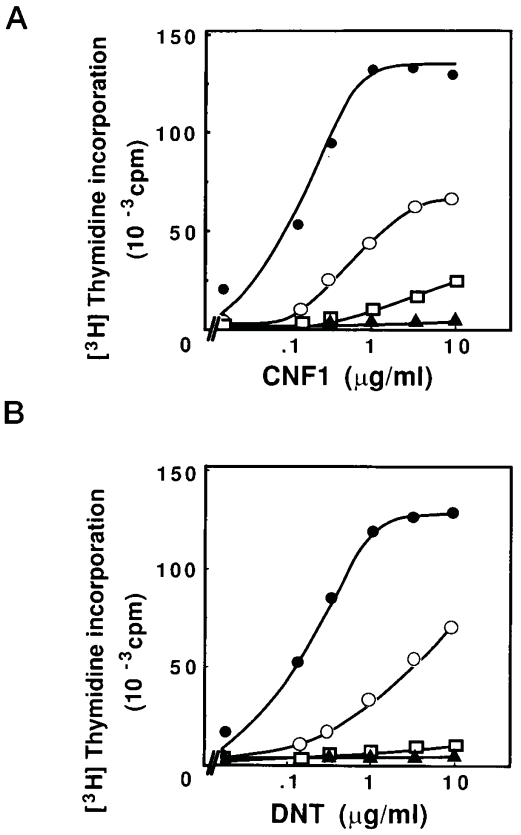

FIG. 5. **Stimulation of DNA synthesis in Swiss 3T3 cells by CNF1 and DNT.** Dose-response curve for the stimulation of DNA synthesis by CNF1 (*A*) and DNT (*B*). Confluent, quiescent cultures of Swiss 3T3 cells were washed and incubated at 37 °C in 2 ml of Dulbecco's modified Eagle's medium DMEM/Waymouth's medium (1:1, v/v), containing 1 μCi of [^{3}H]thymidine/ml. In *panel A*, cultures received various concentrations of the control bacterial lysate (▲) (pGEM3), bacterial lysate containing CNF1 (○), bacterial lysate containing CNF1 and 1 μg/ml insulin (●), or bacterial lysate containing CNF1, 1 μg/ml insulin, and 10 mM CH_3NH_2 (□). In *panel B*, cultures received control bacterial lysate XL1Blue (▲), bacterial lysate containing DNT (○), bacterial lysate containing DNT and 1 μg/ml insulin (●), or bacterial lysate containing DNT, 1 μg of insulin, and 10 mM CH_3NH_2 (□). After 40 h, DNA synthesis was assessed by measuring the level of [^{3}H]thymidine incorporated into half of the acid-precipitable material. Each point is the mean determination from three independent experiments.

2). The control bacterial lysate did not induce actin stress fiber formation or focal adhesion assembly (2–24 h, data not shown).

CNF1-stimulated Tyrosine Phosphorylation Requires Integrity of the Actin Cytoskeleton and Functional $p21^{rho}$—The time-dependent effects of CNF1 on actin stress fiber formation and focal adhesion assembly depicted in Fig. 2 prompted us to examine whether the integrity of the actin cytoskeleton was necessary for CNF1-induced tyrosine phosphorylation. Quiescent cultures of Swiss 3T3 cells were pretreated with 1.2 μM cytochalasin D for 1 h and then stimulated with CNF1 for 6 h. As shown in Fig. 3, cytochalasin D prevented the assembly of focal adhesions (*upper panel C*) and completely blocked tyrosine phosphorylation of $p125^{fak}$ (*middle panel*) and paxillin (data not shown) in response to CNF1.

Recent data from our laboratory have shown that PDGF, at a high concentration (30 ng/ml), completely abolishes bombesin-, lysophosphatidic acid-, and PMT-induced actin stress fiber formation and focal adhesions assembly. Similarly, the marked increase in focal adhesion assembly and actin stress fibers induced by CNF1 was prevented by the addition of PDGF at 30 ng/ml (Fig. 3, *upper panel D*, and results not shown). Since CNF1 stimulated $p125^{fak}$ tyrosine phosphorylation by a mechanism dependent on the integrity of the actin cytoskeleton, we examined whether CNF1-stimulated tyrosine phosphorylation of $p125^{fak}$ could be affected by high concentrations of PDGF. As shown in Fig. 3 (*middle panel*), PDGF (30 ng/ml) markedly reduced CNF1-stimulated tyrosine phosphorylation of $p125^{fak}$.

The *rho* gene product, $p21^{rho}$, has been implicated in the assembly of focal adhesions and in tyrosine phosphorylation of $p125^{fak}$ and paxillin (9, 25, 29, 30). It has been suggested that CNF1 directly targets and activates $p21^{rho}$ (36, 52). To investigate the role of $p21^{rho}$ in the CNF1-stimulated tyrosine phosphorylation of focal adhesion-associated proteins we utilized the *C. botulinum* C3 exoenzyme which ADP-ribosylates Asn^{41} of $p21^{rho}$ and thereby prevents its function (53–55). Recombinant C3 exoenzyme and pure guinea pig IgG were comicroinjected into confluent and quiescent Swiss 3T3 cells, and the cultures were further treated with CNF1 for 4 h. Cells were then fixed, permeabilized, and stained for tyrosine-phosphorylated proteins which are predominantly localized at the focal contacts in CNF1-treated cells (Fig. 3, *lower panel B*). The tyrosine phosphorylation of focal adhesion proteins in response to CNF1 was profoundly inhibited in cells microinjected with C3 exoenzyme (Fig. 3, *lower panel D*). Microinjection itself did not interfere with CNF1-induced tyrosine phosphorylation of focal adhesion proteins (Fig. 3, *lower panels A* and *B*).

CNF1, Unlike PMT, Does Not Induce PKC Activation, Inositol Phosphate Formation, Ca^{2+} Mobilization, or MAPK Activation—PKC activation is a potential signal transduction pathway leading to increased tyrosine phosphorylation of $p125^{fak}$ and paxillin (8). As the effect of CNF1 on PKC activation was unknown, we

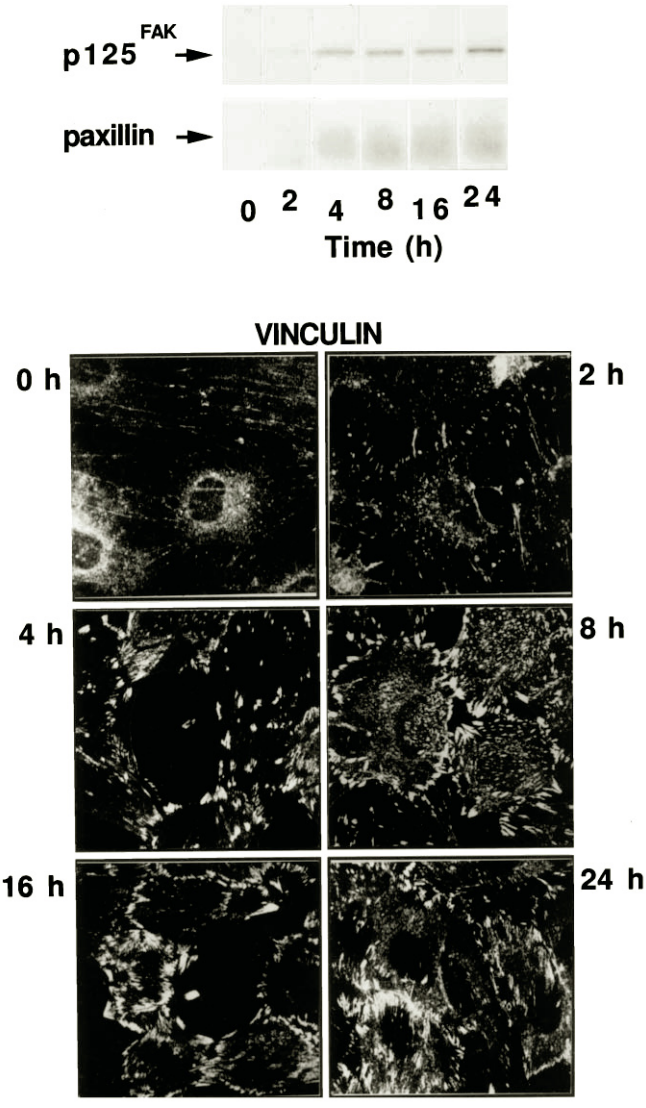

FIG. 6. **DNT induces tyrosine phosphorylation of multiple bands including p125^{fak} and paxillin, and focal adhesion assembly in Swiss 3T3 cells.** *Top*, quiescent cultures of Swiss 3T3 cells were treated in DMEM/Waymouth's medium (1:1, v/v) with 10 μg/ml bacterial lysate containing DNT for various times (0–24 h). Cells were lysed and the lysates were immunoprecipitated with anti-Tyr(P) 4G10 mAb. The immunoprecipitates were fractionated by SDS-PAGE and further analyzed by immunoblotting with p125^{fak} (2A7 mAb) or paxillin (165 mAb). The results shown are representative autoradiographs of at least three independent experiments. *Bottom*, quiescent cultures of Swiss 3T3 cells were washed with DMEM and incubated in DMEM/Waymouth's medium (1:1, v/v) containing 10 μg/ml bacterial lysate containing DNT for the times indicated, and then washed with PBS, fixed in 3.7% paraformaldehyde, and permeabilized with 0.2% Triton X-100. Immunostaining with monoclonal anti-vinculin antibody demonstrates focal adhesions. A Cy3-conjugated rabbit anti-mouse IgG antibody was used to perform confocal imaging. Control bacterial lysate at 10 μg/ml neither induced tyrosine phosphorylation of p125^{fak} and paxillin nor focal adhesion plaques at any of the time points examined (0–24 h, results not shown).

tested whether CNF1 induces phosphorylation of 80K/MARCKS, a major PKC substrate in Swiss 3T3 cells. Cells labeled with [^{32}P]P_i were treated with CNF1 for 6 h and lysed. The lysates were incubated with an anti-80K/MARCKS rabbit polyclonal antibody and the immunoprecipitates were analyzed by SDS-PAGE. As shown in Fig. 4*A*, CNF1 did not stimulate 80K/MARCKS phosphorylation. In contrast, addition of a bacterial lysate containing PMT to parallel cultures induced 80K/MARCKS phosphorylation, in agreement with previous results (56).

To substantiate that CNF1 does not activate a phospholipase C-dependent pathway that leads to the production of the intracellular second messengers diacylglycerol and Ins(1,4,5)P_3, we determined the effect of CNF1 on the production of total inositol phosphates. Quiescent cultures of Swiss 3T3 cells labeled with [2-^{3}H]inositol were incubated with the control bacterial lysate (pGEM3) or with lysate containing CNF1 for 6 h. Fig. 4*B* shows that CNF1 did not stimulate a detectable increase in total inositol phosphate production. In contrast, PMT potently induced the formation of inositol phosphates in parallel cultures of Swiss 3T3 cells.

Prolonged incubation of cells with PMT depletes Ca^{2+} from intracellular stores and thereby prevents Ca^{2+} release by subsequent addition of bombesin (57). To examine whether CNF1 reduces the Ins(1,4,5)P_3-sensitive Ca^{2+} pool in Swiss 3T3 cells, quiescent cultures of these cells were treated with CNF1 or PMT for 4 h, loaded with fura-2-tetraacetoxymethyl ester, and stimulated with 10 nM bombesin. As shown in Fig. 4*C*, treatment with CNF1 did not reduce the Ca^{2+} mobilization induced by subsequent addition of bombesin. In contrast, PMT in parallel cultures caused a dramatic reduction of bombesin-mediated Ca^{2+} mobilization. We conclude that CNF1 stimulates tyrosine phosphorylation through a phospholipase C- and PKC-independent pathway.

Several mitogens stimulate rapid and transient activation of p42^{mapk} and p44^{mapk} through various signal transduction pathways including Ca^{2+} mobilization and PKC activation (58, 59). A significant property of MAPKs activation is the requirement for both Thr and Tyr phosphorylation within its protein kinase subdomain VIII, resulting in a mobility shift in SDS-PAGE gels. To determine if CNF1 induces p42^{mapk} and p44^{mapk} activation, lysates of Swiss 3T3 stimulated for various times with control bacterial lysate (pGEM3), CNF1, or PMT were analyzed by Western blotting with anti-p42^{mapk}/p44^{mapk} antibody. Only PMT induced p42^{mapk} and p44^{mapk} activation as judged by the appearance of slower migrating forms of p42^{mapk} and p44^{mapk} (Fig. 4*D*). We verified that CNF1 failed to stimulate p42^{mapk} and p44^{mapk} activation after various times of incubation (2–6 h).

The striking differences between the early events induced by CNF1 and PMT in Swiss 3T3 cells prompted us to examine the effect of CNF1 on DNA synthesis in these cells. Quiescent cultures of Swiss 3T3 cells were transferred to serum-free medium containing various concentrations of the control bacterial lysate (pGEM3) or CNF1. Cumulative [^{3}H]thymidine incorporation was measured after 40 h. As shown in Fig. 5*A*, CNF1 induced DNA synthesis in a dose-dependent manner whereas the control bacterial lysate (pGEM3) did not induce any measurable increase in [^{3}H]thymidine incorporation in parallel cell cultures. Insulin potentiated the mitogenic effect of CNF1. The maximum levels of DNA synthesis induced by the combination of CNF1 and insulin were similar to those stimulated by medium containing 10% (v/v) fetal bovine serum. Methylamine (10 mM) profoundly inhibited the stimulation of DNA synthesis induced by CNF1 and insulin. Fluorescence-activated cell sorter analysis confirmed that CNF1 stimulated DNA synthesis and induced multinucleation in Swiss 3T3 cells, as described in other cell types (data not shown).

DNT Stimulates p125^{fak} and Paxillin Tyrosine Phosphorylation in a p21^{rho}-dependent Fashion—Recently, DNT from *B. bronchiseptica* has been show to directly target and activate p21^{rho} (37). As shown in Fig. 5*B*, DNT also promotes DNA synthesis in Swiss 3T3 cells. Consequently, we examined whether DNT stimulates a pattern of early events comparable to that induced by CNF1. As shown in Fig. 6, treatment of Swiss 3T3 cells with a bacterial lysate containing DNT stimulated tyrosine phosphorylation of p125^{fak} and paxillin (*upper*

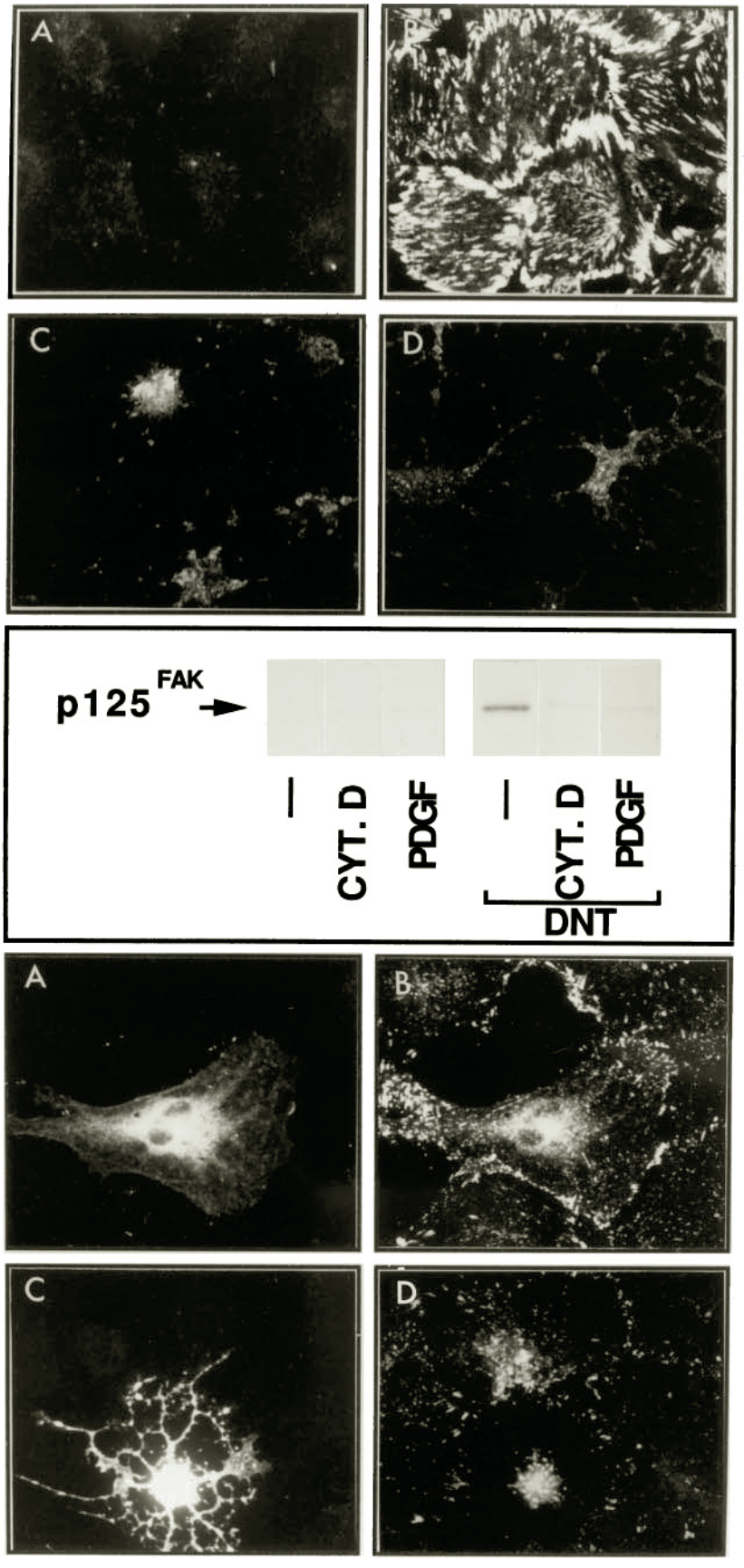

FIG. 7. **Effect of cytochalasin D, PDGF, and C3 exoenzyme on DNT stimulated tyrosine phosphorylation and focal adhesion assembly.** *Upper panel,* effect of cytochalasin D and PDGF on DNT-stimulated focal adhesion assembly. Cells were treated with: (*A*) 10 μg/ml control bacterial lysate (XL1-Blue) for 4 h, (*B*) 10 μg/ml bacterial lysate containing DNT for 4 h, (*C*) 1.2 μM cytochalasin D for 1 h and subsequently with 10 μg/ml bacterial lysate containing DNT for 4 h, or (*D*) 10 μg/ml bacterial lysate containing DNT for 4 h and 30 ng/ml PDGF for a further 10 min. Cells were then washed with PBS and fixed in 4% paraformaldehyde, permeabilized, and focal adhesion were then visualized with mouse anti-vinculin mAb and Cy3-conjugated rabbit anti-mouse IgG. *Middle panel,* effect of cytochalasin D and PDGF on DNT-stimulated $p125^{fak}$ tyrosine phosphorylation. Quiescent Swiss 3T3 cells were treated with (−) 10 μg/ml control bacterial lysate (XL1-Blue) or treated with 1.2 μM cytochalasin D (*CYT.D*) for 1 h and then incubated with 10 μg/ml bacterial lysate containing DNT for a further 4 h. Parallel cell cultures were treated with DNT for 4 h and subsequently with 30 ng/ml PDGF for a further 10 min. Cells were then lysed, and the lysates were further analyzed by immunoprecipitation using mAb 2A7 directed against $p125^{fak}$ followed by anti-Tyr(P) Western blotting. *Lower panel,* microinjection of the C3 exoenzyme prevents the increase of tyrosine phosphorylation of focal adhesion proteins. Quiescent cultures of Swiss 3T3 cells in 30-mm dishes were washed twice and incubated in DMEM/Waymouth's medium (1:1, v/v). Cells were microinjected with 0.5 mg/ml guinea pig IgG (*A* and *B*) or 0.5 mg/ml guinea pig IgG + 100 μg/ml C3 exoenzyme (*C* and *D*). Cells were then treated with 10 μg/ml bacterial lysate containing DNT. After 4 h of incubation, the cells were stained with 4G10 mAb directed against phosphotyrosine residues and visualized by confocal microscopy using Cy3-linked rabbit anti-mouse IgG (*B* and *D*). Microinjected cells (shown in *A* and *B*) were identified by staining with FITC-conjugated goat anti-guinea pig IgG Ab.

panel) with similar kinetics to stress fiber formation (data not shown) and focal adhesion assembly (*lower panel*). The observed lag period suggests that internalization and processing of the toxin in the endosomal/lysosomal compartment is required. Indeed, addition of 10 mM methylamine to the culture medium or reduction of the temperature to 22 °C inhibited

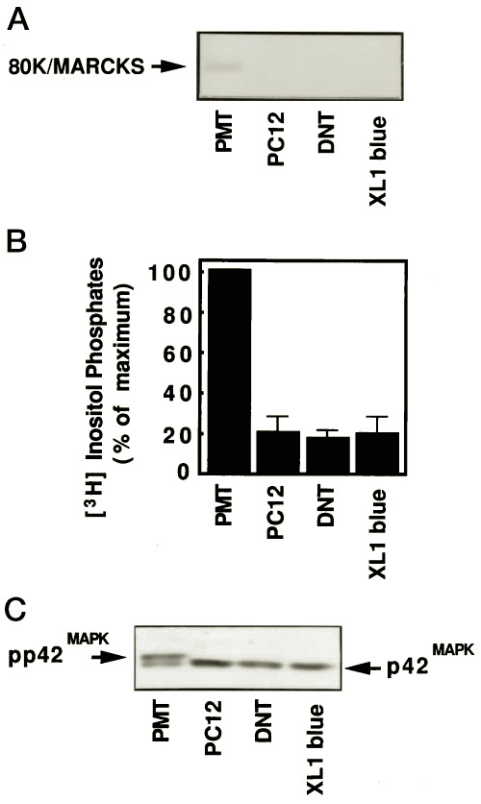

FIG. 8. **DNT does not induce PKC activation, inositol phosphate production, or p42^{mapk} activation**. *A*, quiescent cells, labeled with 50 μCi/ml [^{32}P]P_i for 18 h, were treated with 10 μg/ml control bacterial lysate (XL1-Blue), 10 μg/ml bacterial lysate containing DNT, 2 μg/ml control bacterial lysate (PC12), or 2 μg/ml bacterial lysate containing PMT and incubated for further 6 h. Cells were subsequently lysed and the extracts were immunoprecipitated with anti-80K/MARCKS antibody and further analyzed by SDS-PAGE. *B*, cells were prelabeled with 10 μCi/ml [2-^{3}H]inositol for 16 h and 10 μg/ml control lysate (XL1-Blue), 10 μg/ml bacterial lysate containing DNT, 2 μg/ml control bacterial lysate (PC12), or 2 μg/ml bacterial lysate containing PMT was then added directly to the dishes and the cultures were incubated at 37 °C for 6 h. LiCl (20 mM) was then added, and after a further 30 min the cellular inositol phosphate content was determined. *C*, quiescent cells were treated for 4 h with 10 μg/ml control bacterial lysate (XL1-Blue), 10 μg/ml bacterial lysate containing DNT, 2 μg/ml control bacterial lysate (PC12), or 2 μg/ml bacterial lysate containing PMT and lysed, the lysates were subjected to SDS-PAGE, followed by Western blotting with anti-p42^{mapk} antibody.

DNT-stimulated tyrosine phosphorylation (data not shown).

Next, we tested whether the integrity of the cytoskeleton was necessary for DNT-stimulated tyrosine phosphorylation. As shown in Fig. 7, cytochalasin D or PDGF blocked DNT-stimulated stress fiber formation (data not shown), focal adhesion assembly (*upper panel*), and tyrosine phosphorylation of p125^{fak} (*middle panel*). In addition, microinjection of C3 exoenzyme profoundly inhibited tyrosine phosphorylation of focal adhesion proteins in response to DNT (*lower panel*).

CNF1 stimulates p125^{fak} and paxillin tyrosine phosphorylation and stimulate DNA synthesis without promoting phospholipase C-mediated hydrolysis of PtdIns(4,5)P_2 or PKC activation. As shown in Fig. 8, DNT failed to stimulate an increase in the phosphorylation of 80K/MARCKS or to promote a detectable increase in total inositol phosphate production. In addition, DNT, like CNF1, did not induce p42^{mapk} activation. All these responses were induced by PMT in parallel cultures of Swiss 3T3 cells.

DISCUSSION

The results presented here show for the first time that CNF1 and DNT, both intracellularly acting bacterial toxins, induce tyrosine phosphorylation of multiple substrates in Swiss 3T3 cells. In this study, we identified two substrates, p125^{fak} and paxillin, which were tyrosine phosphorylated in response to CNF1 and DNT. A coordinate increase in tyrosine phosphorylation of p125^{fak} and paxillin is induced by a variety of molecules that regulate cell growth and differentiation (6–9, 11–20, 22). Our results suggest that p125^{fak} and paxillin tyrosine phosphorylation could also play a role in the signaling pathways stimulated by CNF1 and DNT.

Recent findings have raised the possibility that tyrosine phosphorylation of p125^{fak} and paxillin, actin stress fiber formation, focal adhesion assembly, and p21^{rho} function may lie in a novel signal transduction pathway (5, 22, 28, 30) that regulates cell motility and cell proliferation (24, 60). Here we used CNF1 and DNT to examine further the connections predicted by this pathway. We found that CNF1 and DNT stimulated tyrosine phosphorylation of p125^{fak} and paxillin, actin stress fiber formation, and focal adhesion assembly with similar kinetics. Furthermore, pretreatment of quiescent Swiss 3T3 cells with cytochalasin D, at concentrations that completely disrupted the actin cytoskeleton and the focal adhesion plaques, abolished tyrosine phosphorylation of p125^{fak} stimulated by both toxins. These results indicate that integrity of the cytoskeleton is essential for CNF1- and DNT-induced tyrosine phosphorylation. This conclusion was substantiated by experiments using PDGF at a high concentration (30 ng/ml), which disrupted actin stress fibers and focal adhesion assembly in response to CNF1 and DNT. At this concentration PDGF also profoundly decreased CNF1- and DNT-induced tyrosine phosphorylation of p125^{fak}, revealing a novel cross-talk between these toxins and PDGF. Microinjection of *C. botulinum* C3 exoenzyme, which ADP-ribosylates and inactivates p21^{rho} function, prevented tyrosine phosphorylation of focal adhesion proteins in response to either CNF1 or DNT. Thus, our results with CNF1 and DNT provide a novel line of evidence for the existence of a pathway in which p21^{rho} is upstream of cytoskeletal reorganization and tyrosine phosphorylation of p125 and paxillin.

Most extracellular stimuli that promote actin reorganization and tyrosine phosphorylation of p125^{fak} and paxillin also stimulate phospholipase C-mediated hydrolysis of PtdIns(4,5)P_2 leading to Ins(1,4,5)P_3-mediated Ca^{2+} mobilization and to the activation of diacylglycerol-dependent isoforms of PKC. Previous studies indicated that neither Ca^{2+} mobilization nor PKC activation mediate tyrosine phosphorylation of p125^{fak} and paxillin in response to bombesin, lysophosphatidic acid, or PMT (6, 13, 22). However, activated phospholipase C not only generates Ins(1,4,5)P_3 and diacylglycerol but also decreases PtdIns(4,5)P_2 in the plasma membrane. PtdIns(4,5)P_2 binds to several actin-binding proteins and vinculin (61–64) and thereby could modulate the organization of the actin cytoskeleton (65). In addition, p21^{rho} activates phosphatidylinositol-4-phosphate-5-OH kinase and elevates PtdIns(4,5)P_2 synthesis (66). These results raise the possibility that PtdIns(4,5)P_2 turnover may play a role in promoting cytoskeletal reorganization and thus, tyrosine phosphorylation of p125^{fak} and paxillin.

Our results demonstrate that CNF1 and DNT failed to stimulate the formation of inositol phosphates in Swiss 3T3 cells, suggesting that these toxins do not stimulate phospholipase C-mediated PtdIns(4,5)P_2 hydrolysis. This conclusion was substantiated by the inability of CNF1 and DNT to deplete the Ins(1,4,5)P_3-sensitive pool of Ca^{2+} and by the failure of these toxins to stimulate the phosphorylation of 80K/MARCKS, a prominent substrate of diacylglycerol-activated PKC isoforms expressed in Swiss 3T3 cells. In contrast, all these responses were induced by PMT in parallel cultures. Thus, our results demonstrate that p21^{rho}-dependent actin cytoskeleton reorganization, focal adhesion assembly, and tyrosine phosphoryla-

tion of $p125^{fak}$ and paxillin can by dissociated from hydrolysis of PtdIns(4,5)P_2 in CNF1- and DNT-treated Swiss 3T3 cells.

The findings presented here have another interesting implication. A wide range of extracellular signals including growth factors and mitogenic neuropeptides activate one or more members of the family of the highly conserved serine/threonine mitogen-activated protein (MAP) kinases (ERKs) (58, 59, 67). MAP kinases, important intermediates in signal transduction pathways leading to mitogenesis or differentiation, are activated predominantly via PKC in Swiss 3T3 cells stimulated by bombesin. Once activated $p42^{mapk}$ (ERK2) and $p44^{mapk}$ (ERK1) phosphorylate an array of cellular proteins including protein kinases, transcription factors, and proteins involved in the regulation of cell growth (68–71). Because CNF1 and DNT stimulate DNA synthesis in Swiss 3T3 cells, we investigated the ability of these toxins to induce activation of $p42^{mapk}$ and $p44^{mapk}$. Our results demonstrated that unlike PMT, CNF1 and DNT did not stimulate $p42^{mapk}$ in these cells. These results suggest that CNF1 and DNT can signal entry into S phase without activating $p42^{mapk}$ and $p44^{mapk}$ in Swiss 3T3 cells.

The signaling events triggered by CNF and DNT appear to be very similar which suggest that both toxins trigger the same initial event, and indeed there is evidence that CNF and DNT each directly target and modify Rho (36, 37). CNF and DNT are homologous over a region of 100 amino acids near the C terminus (72) which in DNT but not in CNF contains a putative P-loop nucleotide-binding site. We have identified a lysine residue within this motif that is essential for the action of DNT, which suggests that the motif, and by inference this region, is involved in the catalytic function of DNT (51). Thus both CNF and DNT activate Rho but possibly through a different mechanism.

In conclusion, our results with CNF1 and DNT provide further evidence for a $p21^{rho}$-dependent pathway leading to tyrosine phosphorylation of $p125^{fak}$ and paxillin. In particular, actin stress fiber formation, focal adhesion assembly, and tyrosine phosphorylation of $p125^{fak}$ were dissociated from PtdIns(4,5)P_2 hydrolysis in CNF1- and DNT-treated cells. Furthermore, CNF1 and DNT induce DNA synthesis in the absence of detectable activation of $p42^{mapk}$ and $p44^{mapk}$ providing additional evidence for a novel $p21^{rho}$-dependent signaling pathway that leads to entry into the S phase of the cell cycle.

Acknowledgments—We thank Drs. Toni Adams and Isobel Hoskin for production of bacterial lysates and Dr. Alfredo Caprioli for supplying the CNF1 clone.

REFERENCES

1. Hanks, S. K., Calalb, M. B., Harper, M. C., and Patel, S. K. (1992) *Proc. Natl. Acad. Sci. U. S. A.* **89,** 8487–8491
2. Schaller, M. D., Borgman, C. A., Cobb, B. S., Vines, R. R., Reynolds, A. B., and Parsons, J. T. (1992) *Proc. Natl. Acad. Sci. U. S. A.* **89,** 5192–5196
3. Salgia, R., Li, J.-L., Lo, S. H., Brunkhorst, B., Kansas, G. S., Sobhany, E. S., Sun, Y., Pisick, E., Hallek, M., Ernst, T., Tantravahi, R., Chen, L. B., and Griffin, J. D. (1995) *J. Biol. Chem.* **270,** 5039–5047
4. Turner, C. E., and Miller, J. T. (1994) *J. Cell Sci.* **107,** 1583–1591
5. Rozengurt, E. (1995) *Cancer Surveys* **24,** 81–96
6. Zachary, I., Sinnett-Smith, J., and Rozengurt, E. (1992) *J. Biol. Chem.* **267,** 19031–19034
7. Sinnett-Smith, J., Zachary, I., Valverde, A. M., and Rozengurt, E. (1993) *J. Biol. Chem.* **268,** 14261–14268
8. Zachary, I., Sinnett-Smith, J., Turner, C. E., and Rozengurt, E. (1993) *J. Biol. Chem.* **268,** 22060–22065
9. Rankin, S., and Rozengurt, E. (1994) *J. Biol. Chem.* **269,** 704–710
10. Rankin, S., Hooshmand-Rad, R., Claesson-Welsh, L., and Rozengurt, E. (1996) *J. Biol. Chem.* **271,** 7829–7834
11. Kumagai, N., Morii, N., Fujisawa, K., Yoshimasa, T., Nakao, K., and Narumiya, S. (1993) *FEBS Lett.* **329,** 273–276
12. Hordijk, P. L., Verlaan, I., van Corven, E. J., and Moolenaar, W. H. (1994) *J. Biol. Chem.* **269,** 645–651
13. Seufferlein, T., and Rozengurt, E. (1994) *J. Biol. Chem.* **269,** 9345–9351
14. Seufferlein, T., and Rozengurt, E. (1994) *J. Biol. Chem.* **269,** 27610–27617
15. Seufferlein, T., and Rozengurt, E. (1995) *J. Biol. Chem.* **270,** 1–9
16. Kornberg, L., Earp, H. S., Parsons, J. T., Schaller, M., and Juliano, R. L. (1992) *J. Biol. Chem.* **267,** 23439–23442
17. Guan, J. L., and Shalloway, D. (1992) *Nature* **358,** 690–692
18. Burridge, K., Turner, C. E., and Romer, L. H. (1992) *J. Cell Biol.* **119,** 893–903
19. Lipfert, L., Haimovich, B., Schaller, M. D., Cobb, B. S., Parsons, J. T., and Brugge, J. S. (1992) *J. Cell Biol.* **119,** 905–912
20. Vuori, K., and Ruoslahti, E. (1993) *J. Biol. Chem.* **268,** 21459–21462
21. Kanner, S. B., Reynolds, A. B., Vines, R. R., and Parsons, J. T. (1990) *Proc. Natl. Acad. Sci. U. S. A.* **87,** 3328–3332
22. Lacerda, H. M., Lax, A. J., and Rozengurt, E. (1996) *J. Biol. Chem.* **271,** 439–445
23. Schaller, M. D., and Parsons, J. T. (1995) *Mol. Cell. Biol.* **15,** 2635–2645
24. Ilic, D., Furuta, Y., Kanazawa, S., Takeda, N., Sobue, K., Nakatsuji, J., Nomura, S., Fujimoto, J., Okada, M., Yamamoto, T., and Aizawa, S. (1995) *Nature* **377,** 539–544
25. Ridley, A. J., and Hall, A. (1992) *Cell* **70,** 389–399
26. Hynes, R. O. (1992) *Cell* **69,** 11–25
27. Turner, C. E. (1991) *J. Cell Biol.* **115,** 201–207
28. Rankin, S., Morii, N., Narumiya, S., and Rozengurt, E. (1994) *FEBS Lett.* **354,** 315–319
29. Kumagai, N., Morii, N., Fujisawa, K., Nemoto, Y., and Narumiya, S. (1993) *J. Biol. Chem.* **268,** 24535–24538
30. Seckl, M. J., Morii, N., Narumiya, S., and Rozengurt, E. (1995) *J. Biol. Chem.* **270,** 6984–6990
31. Aktories, K., Braun, U., Habermann, B., and Rosener, S. (1990) in *ADP-ribosylating Toxins and G Proteins: Insights into Signal Transduction* (Moss, J., and Vaughn, M., ed) pp. 97–115, American Society for Microbiology, Washington, D. C.
32. Just, I., Wilm, M., Selzer, J., Rex, G., von Eichel-Streiber, C., Mann, M., and Aktories, K. (1995) *J. Biol. Chem.* **270,** 13932–13936
33. Just, I., Selzer, J., Wilm, M., von Eichel-Streiber, C., Mann, M., and Aktories, K. (1995) *Nature* **375,** 500–503
34. Falbo, V., Pace, T., Picci, L., Pizzi, E., and Caprioli, A. (1993) *Infect. Immun.* **61,** 4909–4914
35. Horiguchi, Y., Nakai, T., and Kume, K. (1989) *Microbiol. Pathogens* **6,** 361–368
36. Oswald, E., Sugai, M., Labigne, A., Wu, W., Fiorentini, C., Boquet, P., and O'Brien, A. D. (1994) *Proc. Natl. Acad. Sci. U. S. A.* **91,** 3814–3818
37. Horiguchi, Y., Senda, T., Sugimoto, N., Katahira, J., and Matsuda, M. (1995) *J. Cell Sci.* **108,** 3243–3251
38. Caprioli, A., Falbo, V., Roda, L. G., Ruggeri, F. M., and Zona, C. (1983) *Infect. Immun.* **39,** 1300–1306
39. Caprioli, A., Donelli, G., Falbo, V., Possenti, R., and Roda, L. G. (1984) *Biochem. Biophys. Res. Commun.* **118,** 587–593
40. Horiguchi, Y., Sugimoto, N., and Matsuda, M. (1993) *Infect. Immun.* **61,** 3611–3615
41. Rozengurt, E., and Sinnett-Smith, J. (1983) *Proc. Natl. Acad. Sci. U. S. A.* **80,** 2936–2940
42. Herget, T., Brooks, S. F., Broad, S., and Rozengurt, H. (1993) *Proc. Natl. Acad. Sci U. S. A.* **909,** 2945–2949
43. Kamps, M. P., and Sefton, B. M. (1989) *Anal. Biochem.* **176,** 22–27
44. Erusalimsky, J. D., Brooks, S. F., Herget, T., Morris, C., and Rozengurt, E. (1991) *J. Biol. Chem.* **266,** 7073–7080
45. Berridge, M. J., Dawson, R. M. C., Downes, C. P., Heslop, J. P., and Irvine, R. F. (1983) *Biochem. J.* **212,** 473–482
46. Grynkiewicz, G., Poenie, M., and Tsien, R. Y. (1985) *J. Biol. Chem.* **260,** 3440–3450
47. Lopez-Rivas, A., Mendoza, S. A., Nanberg, E., Sinnett-Smith, J., and Rozengurt, E. (1987) *Proc. Natl. Acad. Sci. U. S. A.* **84,** 5768–5772
48. Nanberg, E., and Rozengurt, E. (1988) *EMBO J.* **7,** 2741–2747
49. Tsien, R. Y., Pozzan, T., and Rink, T. J. (1982) *J. Cell Biol.* **94,** 325–334
50. Leevers, S. J., and Marshall, C. J. (1992) *EMBO J.* **11,** 569–574
51. Pullinger, G. D., Adams, T. E., Mullan, P. B., Garrod, T. I., and Lax, A. J. (1996) *Infect. Immun.* **64,** 4163–4171
52. Fiorentini, C., Donelli, G., Matarrese, P., Fabbri, A., Paradisi, S., and Boquet, P. (1995) *Infect. Immun.* **63,** 3936–3944
53. Nemoto, Y., Namba, T., Kozaki, S., and Narumiya, S. (1991) *J. Biol. Chem.* **266,** 19312–19319
54. Aktories, K., Weller, U., and Chatwal, G. S. (1987) *FEBS Lett.* **212,** 109–113
55. Sekine, A., Fujiwara, M., and Narumiya, S. (1989) *J. Biol. Chem.* **264,** 8602–8605
56. Staddon, J. M., Chanter, N., Lax, A. J., Higgins, T. E., and Rozengurt, E. (1990) *J. Biol. Chem.* **265,** 11841–11848
57. Staddon, J. M., Barker, C. J., Murphy, A. C., Chanter, N., Lax, A. J., Michell, R. H., and Rozengurt, E. (1991) *J. Biol. Chem.* **266,** 4840–4847
58. Pelech, S. L., and Sanghera, J. S. (1992) *Science* **257,** 1355–1356
59. Posada, J., and Cooper, J. A. (1992) *Mol. Biol. Cell* **3,** 383–392
60. Gilmore, A. P., and Romer, L. H. (1996) *Mol. Biol. Cell* **7,** 1209–1224
61. Lee, S. B., and Rhee, S. G. (1995) *Curr. Opin. Cell Biol.* **7,** 183–189
62. Lassing, I., and Lindberg, U. (1985) *Nature* **314,** 472–474
63. Janmey, P. A., and Stossel, T. P. (1987) *Nature* **325,** 362–364
64. Fukami, K. (1992) *Nature* **359,** 150–152
65. Gilmore, A. P., and Burridge, K. (1996) *Nature* **381,** 531–535
66. Chong, L. D., Traynor-Kaplan, A., Bokoch, G. M., and Schwartz, M. A. (1994) *Cell* **79,**
67. Cobb, M., Boulton, T. G., and Robbins, D. J. (1991) *Mol. Biol. Cell* **2,** 965–968
68. Sturgill, T. W., and Wu, J. (1991) *Biochim. Biophys. Acta* **1092,** 350–357
69. Gille, H., Sharrock, A. D., and Shaw, P. E. (1992) *Nature* **358,** 414–417
70. Seth, A., Alvarez, E., Gupta, S., and Davis, R. J. (1991) *J. Biol. Chem.* **266,** 23521–23524
71. Lin, L.-L., Wartman, M., Lin, Y. A., Knopf, J. L., Seth, A., and Davies, R. J. (1993) *Cell* **72,** 269–278
72. Walker, K. E., and Weiss, A. A. (1994) *Infect Immun* **62,** 3817–3828